



Synthesis, characterization and liver targeting evaluation of self-assembled hyaluronic acid nanoparticles functionalized with glycyrrhetic acid



Xiaodan Wang, Xiangqin Gu, Huimin Wang, Yujiao Sun, Haiyang Wu, Shirui Mao*

School of Pharmacy, Shenyang Pharmaceutical University, Shenyang 110016, China

ARTICLE INFO

Article history:

Received 23 June 2016

Received in revised form 8 September 2016

Accepted 26 September 2016

Available online 28 September 2016

Keywords:

Hyaluronic acid

Glycyrrhetic acid

Polymeric nanoparticles

Liver-targeting

ABSTRACT

Recently, polymeric materials with multiple functions have drawn great attention as the carrier for drug delivery system design. In this study, a series of multifunctional drug delivery carriers, hyaluronic acid (HA)-glycyrrhetic acid (GA) succinate (HSG) copolymers were synthesized *via* hydroxyl group modification of hyaluronic acid. It was shown that the HSG nanoparticles had sub-spherical shape, and the particle size was in the range of 152.6–260.7 nm depending on GA graft ratio. HSG nanoparticles presented good short term and dilution stability. MTT assay demonstrated all the copolymers presented no significant cytotoxicity. *In vivo* imaging analysis suggested HSG nanoparticles had superior liver targeting efficiency and the liver targeting capacity was GA graft ratio dependent. The accumulation of DiR (a lipophilic, NIR fluorescent cyanine dye)-loaded HSG-6, HSG-12, and HSG-20 nanoparticles in liver was 1.8-, 2.1-, and 2.9-fold higher than that of free DiR. The binding site of GA on HA may influence liver targeting efficiency. These results indicated that HSG copolymers based nanoparticles are potential drug carrier for improved liver targeting.

© 2016 Published by Elsevier B.V.

1. Introduction

Liver cancer is one of the most prevalent fatal diseases and the morbidity is increasing annually (He et al., 2016). The main drawback of traditional chemotherapy is the high cytotoxicity and indiscriminate distribution in various tissues. Therefore, significant efforts have been exerted towards the design and construction of novel nano-drug delivery systems for better therapy of hepatocytes (Wang et al., 2007; Zhang et al., 2012). Self-assembled nanoparticles, based on polymeric amphiphiles, have generated considerable interests as promising liver-targeted drug delivery carriers because they can solubilize various hydrophobic drugs, improve the *in vivo* stability, prolong drug circulation time in the bloodstream, and meanwhile passively target to tumor tissues by the enhanced permeability and retention (EPR) effect (Elsabhy and Wooley, 2012; Tian et al., 2015). However, passive trapping of nanoparticles still cannot guarantee sufficient drug concentration within the cells, which may lead to inefficient cellular uptake (Choi et al., 2010). To overcome the limitations of passive targeting, a variety of liver targeting moieties such as folic acid (Liu et al., 2011), protein (Krishna et al., 2009), and saccharides (Jiang et al., 2009; Jiang et al., 2011), have been installed on the surface of nanoparticles to further

improve their therapeutic efficacy by receptor-mediated endocytosis (Deng et al., 2012), but this makes the system even more complicated.

Recently, polymeric materials with multiple functions have drawn great attention as the carrier for nanoparticle drug delivery system design (Arpicco et al., 2014; Mahmoudzadeh et al., 2013). It is highly desirable if carrier and active targeting vector can be combined in one material for system simplicity. Hyaluronic acid (HA), composed of repeating disaccharides of N-acetyl-D-glucosamine and D-glucuronic acid, is a promising constituent of nanoparticles due to its high hydrophilicity and targeting ability (Cho et al., 2012; Zou et al., 2013). HA is found in the extracellular matrix and synovial fluids of most human tissues, thus presenting excellent biological properties such as biocompatibility, biodegradability and low toxicity (Arpicco et al., 2014). It is well known HA-binding receptors such as cluster determinant 44 (CD44) (Arpicco et al., 2014; Tripodo et al., 2015), receptor for hyaluronic acid-mediated motility (RHAMM) (Schiffelers et al., 2004) and lymphatic vessel endothelial receptor-1 (LYVE-1) (Bhang et al., 2009) are overexpressed in malignant cells. HA can specifically bind to cancer cells to increase cellular uptake of drugs by receptor-mediated endocytosis and then enhance targeting therefore therapeutic efficacy (Choi et al., 2010).

Glycyrrhetic acid (GA) is an active aglycone of glycyrrhizin and possesses several beneficial pharmacological activities, such as anti-inflammatory, antiviral activity and antiulcerative effect (Lu et al., 2008). GA-mediated drug delivery systems have emerged as novel liver targeting platforms since GA molecules could provide hydrophobic

* Corresponding author at: School of Pharmacy, Shenyang Pharmaceutical University, 103 Wenhua Road, 110016 Shenyang, China.

E-mail address: maoshirui@syphu.edu.cn (S. Mao).

section and liver targeting ligand in combination (Cai et al., 2016; Guo et al., 2013; Tian et al., 2010a). It has been reported that carriers modified with GA have higher accumulation in the liver with superior targeting efficiency to hepatocytes, contributed to the abundant GA receptors on hepatocyte membranes (Tian et al., 2012; Tian et al., 2010b). Furthermore, GA-modified nanoparticles might have the ability to discriminate the normal liver tissue and hepatoma tissue (Tian et al., 2012; Zhang et al., 2012), leading to high therapeutic profile with improved safety.

Therefore, by combining HA and GA in one material via appropriate bridge, using HA as the hydrophilic part and GA as the hydrophobic part, not only the nanoparticles can be prepared by self-assembly process, liver targeting can also be enhanced based on the active targeting capacity originated from both HA and GA. However, although GA could be conjugated on HA by modifying its carboxyl groups with the help of different bridging groups such as ethylenediamine (Zhang et al., 2013a), cystamine (Mezghrani et al., 2015), and adipic dihydrazide (Han et al., 2016), it is realized that the carboxyl groups modification might affect the targeting property of HA because the carboxyl groups are the recognition sites for the enzyme and the receptors (Banerji et al., 2007; Schante et al., 2011). Besides, Tian et al. confirmed that the C₃-hydroxyl group in GA has little influence on the targeting ability (Tian et al., 2010a). Thus, in this paper, our hypothesis is that, conjugating GA to HA via its hydroxyl group modification might achieve better targeting effect. Moreover, considering that GA presents two functions, as the hydrophobic group and meanwhile as the liver targeting ligand, its content might greatly affect the fate of nanoparticles at different stages. How will the GA graft ratio on HA influence the liver targeting efficiency has not been reported so far.

Thus, in this study, first of all, hyaluronic acid-glycyrrhetic acid succinate (HSG) with different graft ratios were synthesized and characterized using ¹H NMR and FT-IR, the physicochemical properties of the self-assembled nanoparticles were characterized using dynamic light scattering (DLS) and transmission electron microscopy (TEM). The cytotoxicity of HSG nanoparticles against HepG2 cells were evaluated using MTT assay. By using DiR as an indicator, liver targeting efficiency of nanoparticles with different GA graft ratio was investigated using a non-invasive near infrared optical imaging technique in mice. To the best of our knowledge, this is the first time that GA was conjugated to HA via hydroxyl group, which may provide better targeting efficiency compared to carboxyl group modification.

2. Materials and methods

2.1. Materials

Hyaluronic acid (HA, 100 kDa) was obtained by oxidative depolymerization (Hokputsa et al., 2003) of HA (200 kDa) supplied by Xian Rongsheng Biotechnology Co. Ltd. (Shanxi, China). Glycyrrhetic acid (GA) was purchased from Nanjing Zelang Medicine Technology Co. Ltd. (Jiangsu, China). Succinic anhydride was from Tianjin Bodi Chemical Holding Co. Ltd. (Tianjin, China). N,N-dicyclohexyl carbodiimide (DCC) and 4-dimethylaminopyridine (DMAP) were from Shanghai Sinopharm Chemical Reagent Co. Ltd. (Shanghai, China). All other chemicals were of analytical grade and were used without further purification.

2.2. Synthesis and characterization of hyaluronic acid-glycyrrhetic acid succinate (HSG) copolymers

Hyaluronic acid-glycyrrhetic acid succinate (HSG) copolymers were synthesized via two steps. Firstly, GA (5.0 mmol), succinic anhydride (20.0 mmol) and DMAP (5.0 mmol) were dissolved in 60 mL of dichloromethane (DCM). The mixture was refluxed at 40 °C for 12 h, then the DCM was removed by evaporation. The precipitate was washed with water, then filtered and dried. The white powder of 3-O-hemisuccinate GA (suc-GA) was obtained by recrystallization in ethanol.

Secondly, to activate its carboxyl group, suc-GA was reacted with DCC and DMAP in 20 mL of dimethylformamide (DMF) at 0 °C for 3 h. The molar ratio of DCC:DMAP:suc-GA was 4:1.33:1. Briefly, HA (200 mg) was dissolved in 10 mL of formamide, followed by addition of different amounts of activated suc-GA. After reacting at 40 °C for 36 h, the solution was dialyzed against dimethylsulfoxide (DMSO) for 2 d and distilled water for 3 d using a dialysis membrane (MWCO: 8000–14,000). The dialyzed solution was filtered and lyophilized to obtain the white, sponge-like HSG copolymers.

The structure of HSG was confirmed by ¹H NMR and FT-IR. ¹H NMR spectra was performed on an AV-600 spectrometer (Bruker, Germany) at room temperature. HA and HSG were dissolved in D₂O and D₂O/DMSO-*d*₆ (1/4, v/v), respectively, whereas GA and suc-GA were dissolved in CDCl₃. FTIR spectra were recorded in the range of 4000 and 400 cm⁻¹ with an IFS-55 spectrometer (Bruker, Switzerland) using KBr pellets. The degree of substitution (DS), defined as the number of GA groups per 100 disaccharide units of HA, was determined by UV-Vis spectrophotometer (UV-2000, Unic, Shanghai, China) at 250 nm (Zhang et al., 2013a). The DS was calculated with the following equation:

$$DS(\%) = \frac{\text{Concentration of GA/Molecular mass of GA}}{(\text{Concentration of HSG-Concentration of GA})/\text{Molecular mass of unit of HA}} \times 100$$

2.3. Determination of critical aggregation concentration (CAC) of HSG

The critical aggregation concentration (CAC) of HSG was determined by fluorescence spectroscopy with pyrene as a probe (Li et al., 2012). Briefly, a known amount of pyrene in acetone was added to a series of 10 mL vials, and acetone was removed by evaporation under nitrogen stream. Then 6 mL of HSG solution in the concentration range from 1×10^{-4} to 1.0 mg/mL, was added to each vial to achieve a final pyrene concentration of 6×10^{-7} M. The solution was sonicated for 30 min and left overnight to equilibrate the pyrene and the nanoparticles. Thereafter, the samples were analyzed by a multimode microplate reader (SpectraMax M3, Molecular Devices, US), with an emission wavelength of 390 nm. The relative excitation fluorescence intensity ratio (I_{338}/I_{334}) was calculated.

2.4. Preparation HSG self-aggregated nanoparticles and DiR-loaded HSG nanoparticles

HSG nanoparticles were prepared by self-assembly in aqueous medium (Yu et al., 2008). Briefly, 10 mg of lyophilized HSG copolymers was dispersed in 10 mL of water (or pH 7.4 PBS to evaluate stability of the nanoparticles) under gentle shaking for 3 h, followed by sonication using a probe-type sonicator (JY92-II, Scientz, Ningbo, China) at 100 W for 10 min under ice bath. Solutions with a concentration of 1 mg/mL were used in the experiment.

The DiR-loaded HSG nanoparticles were prepared by dialysis method (Huo et al., 2012). Briefly, 20 mg of lyophilized HSG was dissolved in 2 mL of formamide and 250 µg of DiR in 250 µL of DMF was added to the above polymer solution. After stirring at room temperature in dark for 24 h, the solution was dialyzed against distilled water for 24 h using a dialysis membrane with a molecular weight cut-off of 8000–14,000. The outer solution was exchanged at 3-h intervals. Subsequently, the dialyzed solution was filtered through a 0.8 µm millipore membrane and then lyophilized.

The amount of DiR in nanoparticles was determined by dissolving the lyophilized nanoparticles in H₂O/DMSO (1/9, v/v) and measuring the absorbance at excitation 748 nm, emission 780 nm using a multimode microplate reader (SpectraMax M3, Molecular Devices, US). The

DiR-loading content (LC) in the nanoparticles was calculated using the following equation:

$$LC(\%) = \frac{\text{The amount of DiR in nanoparticles}}{\text{Total amount of DiR-loaded nanoparticles}} \times 100$$

2.5. Characterization of HSG self-aggregated nanoparticles and DiR-loaded HSG nanoparticles

The particle size of the HSG nanoparticles and DiR-loaded HSG nanoparticles were measured using the Zetasizer (NANOZS90, Malvern Instruments, UK) at 25 °C with a scattering angle of 90°. The zeta potential of the HSG nanoparticles were measured by laser doppler anemometry with the Zetasizer at 25 °C.

Morphology of HSG nanoparticles was observed using transmission electron microscopy (TEM, JEM-2100, Japan) with an accelerating voltage of 200 kV. A drop of the sample solution was placed onto a 300-mesh copper grid with carbon, and then the grid was taped with a filter paper to remove surface water and air-dried. Before visualization, the sample was negatively stained with 2% phosphotungstic acid.

Stability of the HSG nanoparticles upon incubation in PBS (pH 7.4) was studied by monitoring the change of particle size at various incubation times. Similarly stability of the nanoparticles upon dilution was also characterized.

2.6. In vitro cytotoxicity assay

The cytotoxicity of HSG blank nanoparticles against HepG2 cells were evaluated using the MTT (3-(4,5-Dimethylthiazol)-2-yl)-2,5-diphenyltetrazolium bromide) assay (Wang et al., 2014). Briefly, HepG2 cells (5.0×10^3) harvested in a logarithmic growth phase were seeded in 96-well plate and were incubated for 24 h at 37 °C in 5% CO₂. After cell attachment, the cells were incubated with various

concentrations of the HSG blank nanoparticles for 24 h. Then, 20 μL of MTT solution (5.0 mg/mL) was added, and the cells were further incubated for an additional 4 h. Thereafter, the MTT medium was removed from each well, and 150 μL of DMSO was added to dissolve the formazan crystals. Absorbance at 570 nm was measured with a multimode microplate reader (SpectraMax M3, Molecular Devices, US). The untreated cells were taken as a control. Cell viability (%) was calculated as (absorbance of test group/ absorbance of control group) × 100.

2.7. Evaluation of liver targeting effect

For *in vivo* imaging analysis, near infrared fluorescent dye, DiR was incorporated into HSG nanoparticles. All animal studies were approved by the University Ethics Committee of Shenyang Pharmaceutical University and were carried out in accordance with the Principle of Laboratory Animal Care. Twelve hairless Kun Ming (KM) mice were randomly divided into four groups. DiR solution and DiR-loaded HSG nanoparticles were injected into the mice *via* tail vein at a dose of 100 μg DiR/kg. NIRF imaging was taken at 1, 3, 6, 12, and 24 h after injection using an *in vivo* Imaging System (FX, Kodak, USA), in which the excitation and emission wavelengths were 720 nm and 790 nm, respectively. After living imaging, mice were sacrificed and the major organs including liver, lung, spleen, kidney, and heart, were dissected from the mice. And the fluorescence intensity was determined again with the same system as described above.

2.8. Statistical analysis

All data were expressed as means ± SD from at least three separate measurements. A two-tail paired Student's *t*-test was used to compare the difference. Probability value $p < 0.05$ was considered statistically significant.

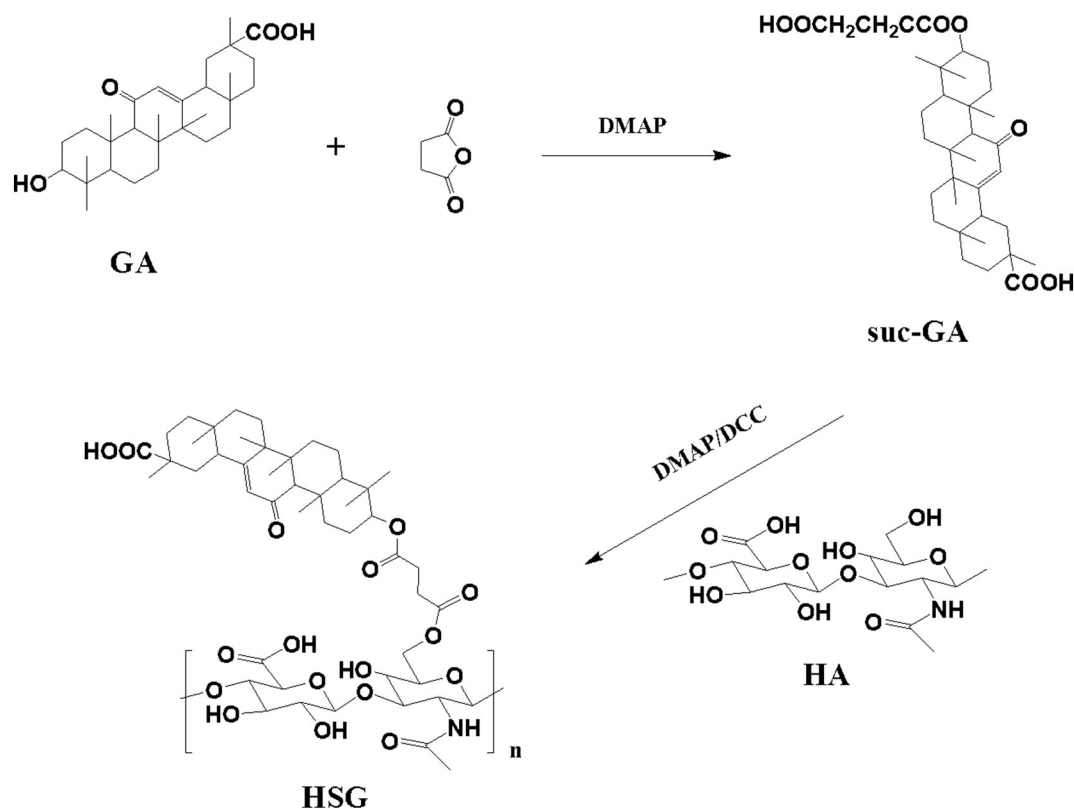


Fig. 1. Synthesis scheme of HSG copolymers.

Table 1
Properties of blank HSG nanoparticles ($n = 3$).

| Sample ^a | Feed ratio (suc-GA/HA) | DS (%) | Size (nm) | PDI | Zeta (mV) | CAC (mg/mL) |
|---------------------|------------------------|------------|--------------|---------------|-------------|-------------|
| HSG-6 | 1/1 | 6.0 ± 0.9 | 260.7 ± 5.4 | 0.102 ± 0.050 | -33.2 ± 1.4 | 0.047 |
| HSG-12 | 1.5/1 | 11.8 ± 1.3 | 213.4 ± 3.5 | 0.098 ± 0.022 | -34.9 ± 0.6 | 0.028 |
| HSG-20 | 2/1 | 20.4 ± 0.7 | 152.6 ± 11.1 | 0.324 ± 0.029 | -37.6 ± 0.7 | 0.020 |

^a HSG-A, in which A represents the degree of substitution (DS).

3. Results and discussion

3.1. Synthesis and characterization of HSG

In this study, in order to retain the carboxyl groups of HA, succinic anhydride was selected as a bridge to couple HA with GA by modifying the hydroxyl group and the synthesis scheme is presented in Fig. 1. Firstly, a carboxyl group was introduced to the C3-hydroxyl group in GA with the help of succinic anhydride, then the carboxyl group of suc-GA was covalently coupled with the hydroxyl group of HA in the presence of DCC and DMAP. Based on the different feed ratio of GA and HA, three HSG copolymers with different GA graft ratio was synthesized, and were coded as HSG-6, HSG-12 and HSG-20, respectively, where the number represents the degree of GA substitution, as presented in Table 1.

The successful synthesis of HSG copolymer was confirmed by ¹H NMR and FT-IR. Fig. 2A exemplifies the ¹H NMR spectra of GA, suc-GA, HA and HSG-12. Compared with GA, a new multiplet at 2.65 ppm observed in the spectrum of suc-GA can be attributed to the two adjacent methylene groups of the succinyl moiety, suggesting that succinyl group was attached to GA successfully. In comparison with HA, the characteristic peaks of GA at 0.8–1.7 ppm, corresponding to the methyl and methylene groups, appeared in the spectrum of HSG-12. It indicated that GA was successfully modified to the structure of HA.

The FTIR spectra of HA and HSG-12 are shown in Fig. 2. Compared with HA, in the spectrum of HSG-12, a new absorption peak emerged at 1729 cm⁻¹, belonging to the new formation of the ester carbonyl group. Simultaneously, the intensity at 2930–2850 cm⁻¹ was enhanced sharply in the spectrum of HSG-12, which can be attributed to the carbon-to-hydrogen stretching vibrations from the large number of methyl and methylene groups of GA moiety of HSG-12, further suggesting that GA has been attached to HA backbone successfully.

3.2. Influence of GA graft ratio on the critical aggregation concentration of HSG

A remarkably low CAC is crucial for nanoparticles since lower CAC value can provide better resistance to particle dissociation upon extreme dilution in blood, thus allowing prolonged circulation time before reaching the targeting site (Mahmoudzadeh et al., 2013). In this study, the CAC of HSG copolymer was determined by fluorescence spectroscopy and pyrene was chosen as a fluorescent probe because it can preferably locate inside the hydrophobic inner core of nanoparticles (Yu et al., 2008). When the nanoparticles were formed, the intensity ratio I₃₃₈/I₃₃₄ of the pyrene excitation spectra varied substantially, reflecting the transfer of pyrene from the aqueous environment to the hydrophobic domains (Xiangyang et al., 2007). As shown in Table 1, the CAC value of HSG copolymers was GA substitution dependent, since higher hydrophobicity could form the inner core of nanoparticles more readily. It decreased remarkably when increasing GA content from 6% to 12%, with the CAC value 0.047, and 0.028 mg/mL respectively, and further increasing GA graft ratio to 20% caused a slight decrease of CAC value, from 0.028 mg/mL for HSG-12 to 0.020 mg/mL for HSG-20, implying a good hydrophilic and lipophile balance has been achieved at this ratio. This result implies that HSG nanoparticles with the relatively low CAC value may have good stability under highly diluted condition after intravenous injection.

3.3. Preparation and characterization of blank HSG self-aggregated nanoparticles

The blank HSG nanoparticles were prepared by self-assembly process in aqueous medium. The particle sizes and the zeta potentials of various blank HSG nanoparticles are listed in Table 1. It was noted that

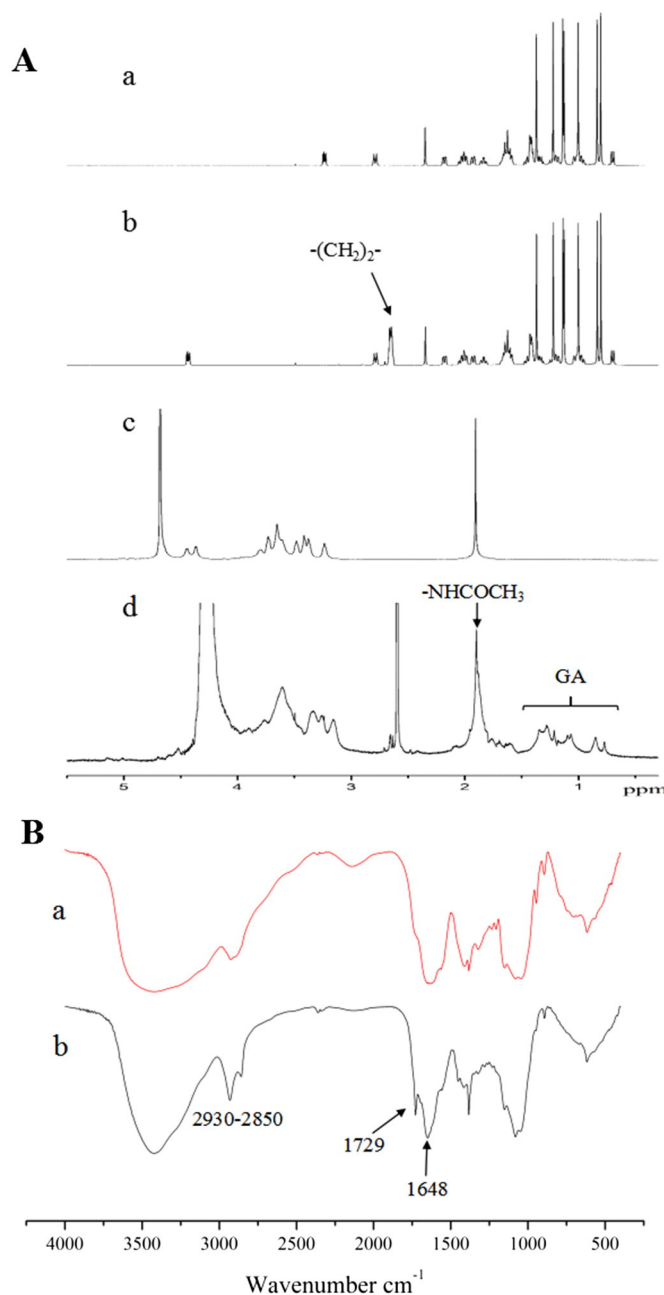


Fig. 2. (A) ¹H NMR spectra of GA (a), suc-GA (b), HA (c) and HSG-12 (d), and (B) FTIR spectra of HA (a) and HSG-12(b).

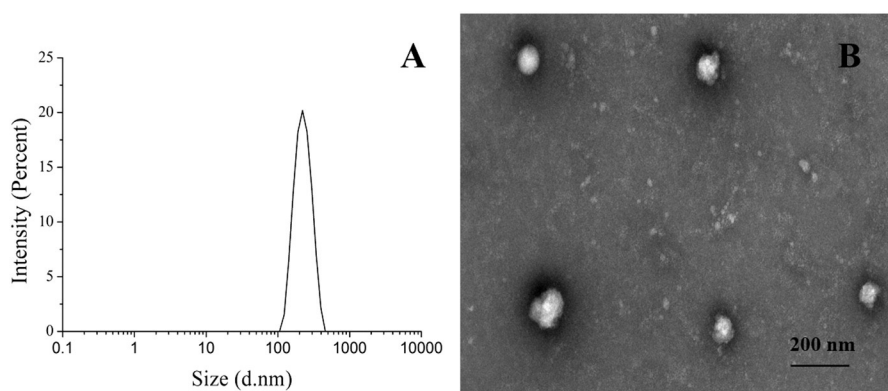


Fig. 3. Particle size distribution measured by dynamic light scattering (DLS) (A) and TEM image (B) of the HSG-12 nanoparticles.

the size of HSG nanoparticles decreased with the increase of GA graft ratio and it decreased from 260 nm to 152 nm when GA ratio increased from 6% to 20%. This can probably be explained by the enhanced hydrophobic interaction among glycyrrhetic acid groups, making the inner core more compacted, therefore smaller particle size. A similar tendency was reported previously (Li et al., 2012). As for particle size distribution, unimodal size distribution was found for HSG-6 and HSG-12 nanoparticles (Fig. 5A) and it has a tendency to be broader for HSG-20 nanoparticles due to the smaller size. All the HSG nanoparticles were negatively charged with zeta potential value in the range of -33.2 to -37.6 mV, which may attribute to the presence of ionized carboxylic groups of HA on the surface of the nanoparticles. Such high surface charge may provide an electrostatic repelling force among the particles, therefore increasing the nanoparticle stability. In addition, negatively charged nanoparticles are reported to be able to contribute to efficacious evasion of the renal filtration (Elsabhy and Wooley, 2012).

Transmittance scanning electron microscopy (TEM) was used to directly visualize the size and morphology of HSG nanoparticles. As shown in Fig. 3B, HSG-12 nanoparticles had an almost spherical shape and the observed particle size was approximately 100 nm, which was smaller than the hydrodynamic diameter obtained by DLS. This discrepancy might be due to the different sample preparation technologies. DLS measurements were carried out under aqueous condition, but TEM images were obtained for dried samples with the shrinkage of hydrophilic shell of nanoparticles (Han et al., 2011).

3.4. Stability of HSG self-aggregated nanoparticles

Dilution of polymeric nanoparticles upon *in vivo* administration may lead to premature dissociation, drug release, and therefore low tumor-targeting ability (Deng et al., 2012; Elsabhy and Wooley, 2012). Therefore, for clinical application, the stability of nanoparticles is of special importance for long term blood circulation to guarantee better therapeutic effect. First of all, short term stability of the nanoparticles *in vitro* was investigated using evolution of particle size as a criterion. As shown in Fig. 4A, HSG nanoparticles could maintain their size unchanged in PBS (pH 7.4) for at least 6 days, indicating good thermodynamic stability of the nanoparticles in aqueous media. And then the stability of the nanoparticles upon dilution was characterized and shown in Fig. 4B. It was found the particle size had no significant change towards 10-times dilution compared to the original nanoparticles ($p > 0.05$). These facts indicated that HSG nanoparticles had a good stability, probably attributed to its low CAC and high surface charge.

3.5. *In vitro* cytotoxicity of HSG nanoparticles

For clinical application, ideally, carriers developed for drug delivery should exhibit low toxicity and high biocompatibility (Zhang et al., 2013b). It is well known that hyaluronic acid, present in the

extracellular matrix and synovial fluids of most human tissues, has excellent biological properties (Arpicco et al., 2014; Tripodo et al., 2015), but the toxicity of novel HSG carriers is not clear. Therefore, MTT assays were performed to test the effect of self-assembled HSG polymeric nanoparticles on the metabolic activity of cells. The cellular viability of HSG nanoparticles against HepG2 is shown in Fig. 5. It was found that the average cell viability of blank HSG nanoparticles was $>89\%$, indicating all the copolymers present no significant cytotoxicity and have good biocompatibility to the cells.

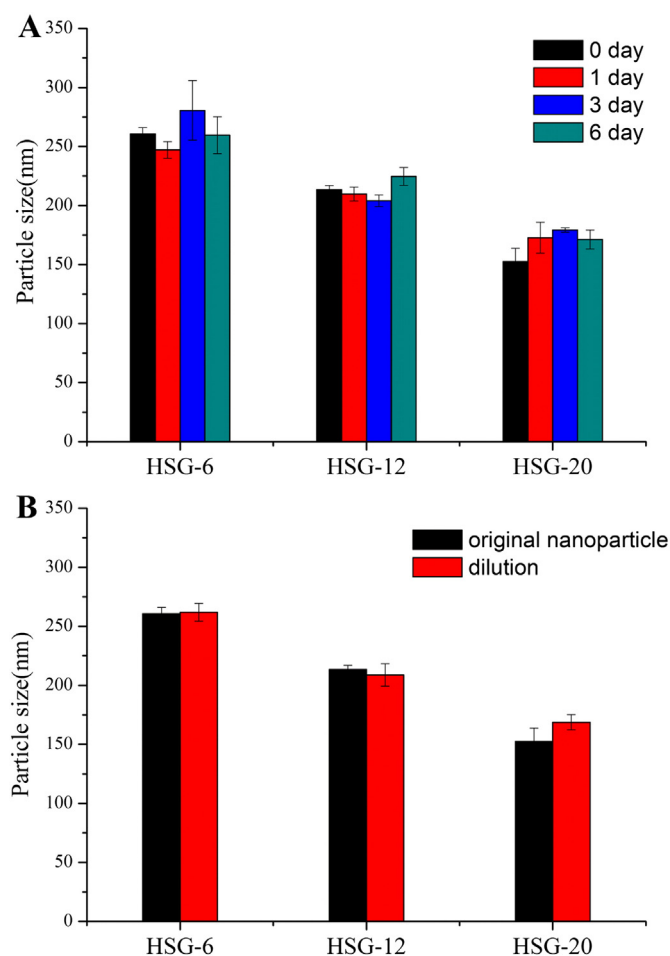


Fig. 4. The stability of HSG nanoparticles at various incubation time (A) and towards dilution (B) ($n = 3$).

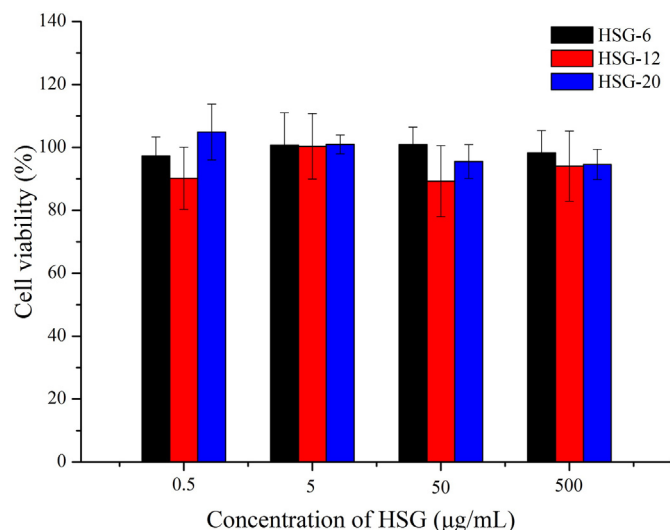


Fig. 5. *In vitro* cytotoxicity of HSG nanoparticles against HepG2 cells after incubation for 24 h ($n = 6$).

3.6. Liver-targeting properties of nanoparticle observed by *in vivo* imaging

To evaluate *in vivo* tissue distribution and liver-targeting ability of HSG nanoparticles, DiR was selected as a NIR fluorescent dye and was investigated using a NIR fluorescence imaging technique. The amount of DiR in HSG-6, HSG-12, and HSG-20 nanoparticles was calculated to be 0.87%, 0.95%, and 1.03%, respectively, and the particle sizes were 257.6, 231.1, and 168.9 nm, respectively ($n = 3$). After loading the DiR, the particle sizes showed no significant change compared to those of corresponding blank nanoparticles ($p > 0.05$).

The real-time images of free DiR and DiR-labeled HSG nanoparticles are shown in Fig. 6A. For the free DiR group, a weak fluorescence signal was detected 1 h after drug delivery, the intensity was the strongest at

3 h and started to decrease gradually thereafter, and nothing is visible after 24 h. In contrast, much stronger fluorescence signal in the liver region was observed for various HSG nanoparticles tested and the highest intensity level was achieved at 12 h. Moreover, it was found that the liver targeting efficiency was significantly affected by the DS of GA, and HSG-20 nanoparticle had considerable strong fluorescence signal even at 24 h after injection, compared to only 12 h for HSG-6 based nanoparticles. As shown in Fig. 6C, the *ex vivo* fluorescent image of excised organs further confirmed that DiR-labeled HSG nanoparticles showed higher fluorescence accumulation in the liver compared with free DiR and the GA content had significant effect on the liver targeting ability. Quantitative analyses (Fig. 6B) indicated that the fluorescence intensity of HSG-6, HSG-12, and HSG-20 nanoparticles in liver was 1.8-, 2.1-, and 2.9-fold higher than that of free DiR, respectively.

It is well known that the particle size may influence the biodistribution of nanoparticles in body as well (Hickey et al., 2015). In the liver, the size of the fenestrations in the hepatic endothelium is 100–150 nm in diameter (Gaumet et al., 2008; Moghimi et al., 2001), and carrier systems with diameters of 150–300 nm can induce nonspecific RES uptake (Gaumet et al., 2008). In our work, three DiR-labeled HSG nanoparticles (160–260 nm) could be taken up by the RES cells present in the liver. But it seems that the particle size was not the main reason for the different accumulation in liver. Tian et al. prepared glycyrrhetic acid-modified chitosan/poly(ethylene glycol) nanoparticles with the similar particle size as we reported here (Tian et al., 2010a), and the nanoparticles also presented an increasing liver targeting ability as the GA content increased, further indicating that the distinct difference in body distribution is not related to the difference in particle size.

Glycyrrhetic acid, the hydrophobic group, is anticipated to exist inside the inner core when nanoparticles are formed. However, Park et al. prepared folate-mediated MPEG/PCL nanospheres and theoretically, folate groups should be included into the inner cores, because folate was coupled with the terminal hydrophobic PCL block. But the XPS results evidenced that some folate existed on the surface of the nanospheres (Park et al., 2005). Chiu et al. also confirmed that palmitoyl groups existed both on the surface and inside of the N-palmitoyl chitosan

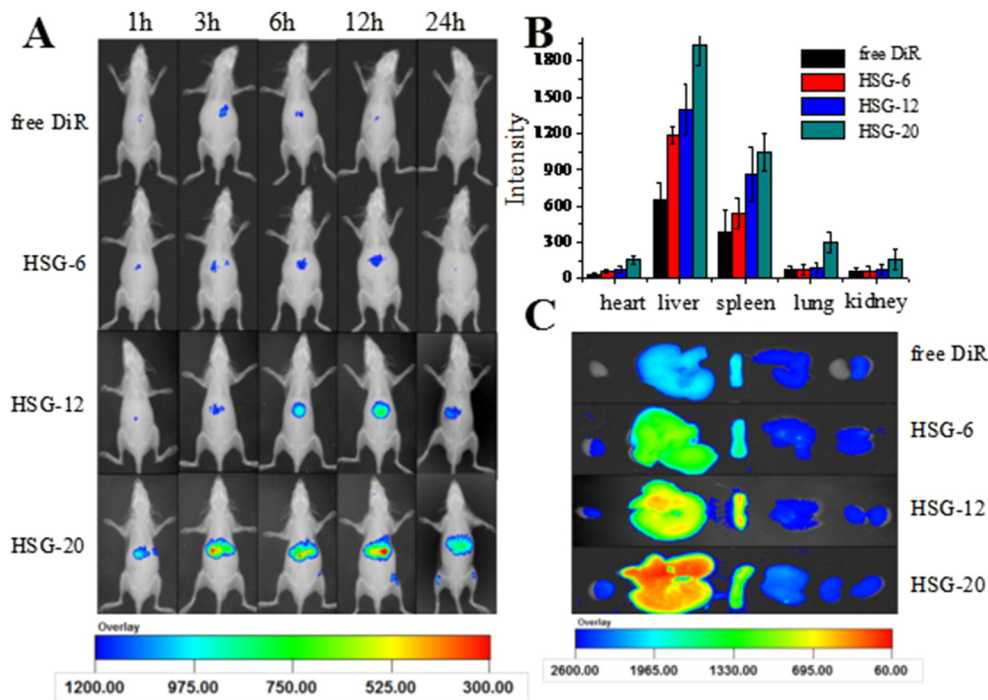


Fig. 6. Fluorescence imaging of KM mice after administration of free DiR and DiR-loaded HSG nanoparticles, respectively. (A) Time-dependent *in vivo* images after i.v. injection. (B) *Ex vivo* fluorescence images of tissues at 24 h post-injection. (C) Quantification of the *ex vivo* tissue uptake characteristics after 24 h post-injection ($n = 3$).

Table 2

Properties comparison of hyaluronic acid-graft-glycyrrhetic acid nanoparticles with different bridging groups.

| Sample | Binding site | Bridging group | DS (%) | CAC (mg/mL) | Size (nm) | liver targeting ability |
|------------------|-----------------|-----------------|--------|-------------|--------------|--|
| HA-Suc-GA (HSG) | Hydroxyl groups | Succinic acid | 20.4 | 0.020 | 152.6 ± 11.1 | 2.9-fold higher than that of free DiR at 24 h |
| HA-Etda-GA (HGA) | Carboxyl groups | Ethylenediamine | 20.2 | 0.078 | 203.4 ± 2.2 | 1.8-fold higher than that of free DiR at 24 h (Zhang et al., 2013a) |
| HA-Cyst-GA | Carboxyl groups | Cystamine | 23.8 | 0.035 | 190.9 ± 0.5 | 1.8-fold higher than that of free DiR at 12 h (Mezghrani et al., 2015) |

nanoparticles and with the DS increase of palmitoyl groups, there were more palmitoyl groups present on the surface of nanoparticles (Chiu et al., 2010). Based on these results, it is reasonable to assume that in the HSG nanoparticles prepared in our study, GA molecules were partially exposed on the surface of the particles. And this is in good agreement with our experimental data. The larger the GA content, the higher density of GA on the surfaces of the nanoparticles, which could lead to higher binding affinity to the liver region by GA receptor-mediated endocytosis.

In the past, most studies have been devoted to the specific ligand-decoration of nanoparticles for targeted drug delivery to the liver or the treatment of hepatocellular carcinoma (Jiang et al., 2009; Liu et al., 2011). In this study, interestingly, we found that the binding site might have a certain effect on the targeting properties of nanoparticles. As shown in Table 2, with the similar DS of GA, HSG nanoparticles synthesized by modifying the hydroxyl groups as presented in this study had smaller size, lower CAC value and higher liver targeting capacity compared with that of nanoparticles synthesized by modifying carboxyl groups (Mezghrani et al., 2015; Zhang et al., 2013a). Therefore, coupling HA with GA by modifying hydroxyl groups might provide better physicochemical properties and high targeting efficiency compared to carboxyl group modification. Overall, HSG nanoparticles could be expected to be a high efficient drug delivery vehicle to achieve liver-targeting.

4. Conclusion

A multifunctional drug delivery carrier based on hyaluronic acid-glycyrrhetic acid succinate (HSG) nanoparticles was synthesized successfully in this study. This novel HA derivative could self-assemble into nanoparticles in aqueous solution. *In vitro* studies showed HSG nanoparticles had a good stability and presented no significant cytotoxicity. *In vivo* investigation confirmed that HSG nanoparticles had superior targeting efficiency to liver and the liver targeting capacity was significantly affected by the DS of GA. The accumulation of DiR-loaded HSG-6, HSG-12, and HSG-20 nanoparticles in liver was 1.8-, 2.1-, and 2.9-fold higher than that of free DiR. These results indicated that HSG nanoparticles have great potential as liver-targeted carriers for biomedical applications.

Acknowledgments

This project is financially supported by the National Natural Science Foundation of China (Grant No. 81273446) and Liaoning Institutions excellent talents support plan (No. LR2013047).

References

Arpicco, S., Milla, P., Stella, B., Dosio, F., 2014. Hyaluronic acid conjugates as vectors for the active targeting of drugs, genes and Nanocomposites in cancer treatment. *Molecules* 19, 3193–3230.

Banerji, S., Wright, A.J., Noble, M., Mahoney, D.J., Campbell, I.D., Day, A.J., Jackson, D.G., 2007. Structures of the Cd44-hyaluronan complex provide insight into a fundamental carbohydrate-protein interaction. *Nat. Struct. Mol. Biol.* 14, 234–239.

Bhang, S.H., Won, N., Lee, T.-J., Jin, H., Nam, J., Park, J., Chung, H., Park, H.-S., Sung, Y.-E., Hahn, S.K., Kim, B.-S., Kim, S., 2009. Hyaluronic acid-quantum dot conjugates for *in vivo* lymphatic vessel imaging. *ACS Nano* 3, 1389–1398.

Cai, Y., Xu, Y., Chan, H.F., Fang, X., He, C., Chen, M., 2016. Glycyrrhetic acid mediated drug delivery carriers for hepatocellular carcinoma therapy. *Mol. Pharm.* 13, 699–709.

Chiu, Y.-L., Ho, Y.-C., Chen, Y.-M., Peng, S.-F., Ke, C.-J., Chen, K.-J., Mi, F.-L., Sung, H.-W., 2010. The characteristics, cellular uptake and intracellular trafficking of nanoparticles made of hydrophobically-modified chitosan. *J. Control. Release* 146, 152–159.

Cho, H.-J., Yoon, I.-S., Yoon, H.Y., Koo, H., Jin, Y.-J., Ko, S.-H., Shim, J.-S., Kim, K., Kwon, I.C., Kim, D.-D., 2012. Polyethylene glycol-conjugated hyaluronic acid-ceramide self-assembled nanoparticles for targeted delivery of doxorubicin. *Biomaterials* 33, 1190–1200.

Choi, K.Y., Chung, H., Min, K.H., Yoon, H.Y., Kim, K., Park, J.H., Kwon, I.C., Jeong, S.Y., 2010. Self-assembled hyaluronic acid nanoparticles for active tumor targeting. *Biomaterials* 31, 106–114.

Deng, C., Jiang, Y.J., Cheng, R., Meng, F.H., Zhong, Z.Y., 2012. Biodegradable polymeric micelles for targeted and controlled anticancer drug delivery: promises, progress and prospects. *Nano Today* 7, 467–480.

Elsabhy, M., Wooley, K.L., 2012. Design of polymeric nanoparticles for biomedical delivery applications. *Chem. Soc. Rev.* 41, 2545–2561.

Gaument, M., Vargas, A., Gurny, R., Delie, F., 2008. Nanoparticles for drug delivery: the need for precision in reporting particle size parameters. *Eur. J. Pharm. Biopharm.* 69, 1–9.

Guo, H., Lai, Q., Wang, W., Wu, Y., Zhang, C., Liu, Y., Yuan, Z., 2013. Functional alginate nanoparticles for efficient intracellular release of doxorubicin and hepatoma carcinoma cell targeting therapy. *Int. J. Pharm.* 451, 1–11.

Han, S.-Y., Han, H.S., Lee, S.C., Kang, Y.M., Kim, I.-S., Park, J.H., 2011. Mineralized hyaluronic acid nanoparticles as a robust drug carrier. *J. Mater. Chem.* 21, 7996–8001.

Han, X., Wang, Z., Wang, M., Li, J., Xu, Y., He, R., Guan, H., Yue, Z., Gong, M., 2016. Liver-targeting self-assembled hyaluronic acid-glycyrrhetic acid micelles enhance hepato-protective effect of silybin after oral administration. *Drug Delivery* 23, 1818–1829.

He, Z.X., Xiang, P., Gong, J.P., Cheng, N.S., Zhang, W., 2016. Radiofrequency ablation versus resection for Barcelona clinic liver cancer very early/early stage hepatocellular carcinoma: a systematic review. *Ther. Clin. Risk Manag.* 12, 295–303.

Hickey, J.W., Santos, J.L., Williford, J.-M., Mao, H.-Q., 2015. Control of polymeric nanoparticle size to improve therapeutic delivery. *J. Control. Release* 219, 536–547.

Hokpusta, S., Jumel, K., Alexander, C., Harding, S.E., 2003. Hydrodynamic characterisation of chemically degraded hyaluronic acid. *Carbohydr. Polym.* 52, 111–117.

Huo, M., Zou, A., Yao, C., Zhang, Y., Zhou, J., Wang, J., Zhu, Q., Li, J., Zhang, Q., 2012. Somatostatin receptor-mediated tumor-targeting drug delivery using octreotide-PEG-deoxycholic acid conjugate-modified N-deoxycholic acid-O, N-hydroxyethylation chitosan micelles. *Biomaterials* 33, 6393–6407.

Jiang, H.-L., Kim, Y.-K., Arote, R., Jere, D., Quan, J.-S., Yu, J.-H., Choi, Y.-J., Nah, J.-W., Cho, M.-H., Cho, C.-S., 2009. Mannosylated chitosan-graft-polyethylenimine as a gene carrier for Raw 264.7 cell targeting. *Int. J. Pharm.* 375, 133–139.

Jiang, H., Wu, H., Xu, Y.-L., Wang, J.-z., Zeng, Y., 2011. Preparation of galactosylated chitosan/tripolyphosphate nanoparticles and application as a gene carrier for targeting SMMC7721 cells. *J. Biosci. Bioeng.* 111, 719–724.

Krishna, A.D.S., Mandraju, R.K., Kishore, G., Kondapi, A.K., 2009. An efficient targeted drug delivery through apotransferrin loaded nanoparticles. *PLoS One* 4, e7240.

Li, J., Huo, M., Wang, J., Zhou, J., Mohammad, J.M., Zhang, Y., Zhu, Q., Waddad, A.Y., Zhang, Q., 2012. Redox-sensitive micelles self-assembled from amphiphilic hyaluronic acid-deoxycholic acid conjugates for targeted intracellular delivery of paclitaxel. *Biomaterials* 33, 2310–2320.

Liu, Y.H., Sun, J., Cao, W., Yang, J.H., Lian, H., Li, X., Sun, Y.H., Wang, Y.J., Wang, S.L., He, Z.G., 2011. Dual targeting folate-conjugated hyaluronic acid polymeric micelles for paclitaxel delivery. *Int. J. Pharm.* 421, 160–169.

Lu, Y., Li, J., Wang, G., 2008. *In vitro* and *in vivo* evaluation of mPEG-PLA modified liposomes loaded glycyrrhetic acid. *Int. J. Pharm.* 356, 274–281.

Mahmoudzadeh, M., Fassihi, A., Emami, J., Davies, N.M., Dorkoosh, F., 2013. Physicochemical, pharmaceutical and biological approaches toward designing optimized and efficient hydrophobically modified chitosan-based polymeric micelles as a nanocarrier system for targeted delivery of anticancer drugs. *J. Drug Target.* 21, 693–709.

Mezghrani, O., Tang, Y., Ke, X., Chen, Y., Hu, D., Tu, J., Zhao, L., Bourkaib, N., 2015. Hepatocellular carcinoma dually-targeted nanoparticles for reduction triggered intracellular delivery of doxorubicin. *Int. J. Pharm.* 478, 553–568.

Moghim, S.M., Hunter, A.C., Murray, J.C., 2001. Long-circulating and target-specific nanoparticles: theory to practice. *Pharmacol. Rev.* 53, 283–318.

Park, E.K., Lee, S.B., Lee, Y.M., 2005. Preparation and characterization of methoxy poly(ethylene glycol)/poly(epsilon-caprolactone) amphiphilic block copolymeric nanospheres for tumor-specific folate-mediated targeting of anticancer drugs. *Biomaterials* 26, 1053–1061.

Schante, C.E., Zuber, G., Herlin, C., Vandamme, T.F., 2011. Chemical modifications of hyaluronic acid for the synthesis of derivatives for a broad range of biomedical applications. *Carbohydr. Polym.* 85, 469–489.

Schiffelers, R.M., Ansari, A., Xu, J., Zhou, Q., Tang, Q.Q., Storm, G., Molema, G., Lu, P.Y., Scaria, P.V., Woodle, M.C., 2004. Cancer siRNA therapy by tumor selective delivery with ligand-targeted sterically stabilized nanoparticle. *Nucleic Acids Res.* 32, e149.

Tian, Q., Wang, X., Wang, W., Zhang, C., Liu, Y., Yuan, Z., 2010a. Insight into glycyrrhetic acid: the role of the hydroxyl group on liver targeting. *Int. J. Pharm.* 400, 153–157.

- Tian, Q., Zhang, C.-N., Wang, X.-H., Wang, W., Huang, W., Cha, R.-T., Wang, C.-H., Yuan, Z., Liu, M., Wan, H.-Y., Tang, H., 2010b. Glycyrrhetic acid-modified chitosan/poly(ethylene glycol) nanoparticles for liver-targeted delivery. *Biomaterials* 31, 4748–4756.
- Tian, Q., Wang, X.H., Wang, W., Zhang, C.N., Wang, P., Yuan, Z., 2012. Self-assembly and liver targeting of sulfated chitosan nanoparticles functionalized with glycyrrhetic acid. *Nanomedicine: nanotechnology, biology, and medicine* 8, 870–879.
- Tian, Y., Shi, C., Sun, Y., Zhu, C., Sun, C.C., Mao, S., 2015. Designing micellar nanocarriers with improved drug loading and stability based on solubility parameter. *Mol. Pharm.* 12, 816–825.
- Tripodo, G., Trapani, A., Torre, M.L., Giammona, G., Trapani, G., Mandracchia, D., 2015. Hyaluronic acid and its derivatives in drug delivery and imaging: recent advances and challenges. *Eur. J. Pharm. Biopharm.* 97, 400–416.
- Wang, Y., Yu, L., Han, L., Sha, X., Fang, X., 2007. Difunctional Pluronic copolymer micelles for paclitaxel delivery: synergistic effect of folate-mediated targeting and Pluronic-mediated overcoming multidrug resistance in tumor cell lines. *Int. J. Pharm.* 337, 63–73.
- Wang, L., Li, L., Sun, Y., Ding, J., Li, J., Duan, X., Li, Y., Junyaprasert, V.B., Mao, S., 2014. In vitro and in vivo evaluation of chitosan graft glyceryl monooleate as peroral delivery carrier of enoxaparin. *Int. J. Pharm.* 471, 391–399.
- Xiangyang, X., Ling, L., Jianping, Z., Shiyue, L., Jie, Y., Xiaojin, Y., Jinsheng, R., 2007. Preparation and characterization of N-succinyl-N'-octyl chitosan micelles as doxorubicin carriers for effective anti-tumor activity. *Colloids and surfaces. B, Biointerfaces* 55, 222–228.
- Yu, J.-M., Li, Y.-H., Qiu, L.-Y., Jin, Y., 2008. Self-aggregated nanoparticles of cholesterol-modified glycol chitosan conjugate: preparation, characterization, and preliminary assessment as a new drug delivery carrier. *Eur. Polym. J.* 44, 555–565.
- Zhang, C., Wang, W., Liu, T., Wu, Y., Guo, H., Wang, P., Tian, Q., Wang, Y., Yuan, Z., 2012. Doxorubicin-loaded glycyrrhetic acid-modified alginate nanoparticles for liver tumor chemotherapy. *Biomaterials* 33, 2187–2196.
- Zhang, L., Yao, J., Zhou, J., Wang, T., Zhang, Q., 2013a. Glycyrrhetic acid-graft-hyaluronic acid conjugate as a carrier for synergistic targeted delivery of antitumor drugs. *Int. J. Pharm.* 441, 654–664.
- Zhang, N., Wardwell, P.R., Bader, R.A., 2013b. Polysaccharide-based micelles for drug delivery. *Pharmaceutics* 5, 329–352.
- Zou, A., Chen, Y., Huo, M., Wang, J., Zhang, Y., Zhou, J., Zhang, Q., 2013. In vivo studies of octreotide-modified N-octyl-O, N-carboxymethyl chitosan micelles loaded with doxorubicin for tumor-targeted delivery. *J. Pharm. Sci.* 102, 126–135.